REFLECTION OF A HIGH-CURRENT ELECTRON BEAM FROM A PLASMA LAYER WITH A DIFFUSE BOUNDARY

O. G. Antanblyan, V. P. Grigor'ev,
A. G. Potashev, L. V. Presler,
and E. K. Khanikyants

UDC 533.951

The problem of the interaction of high-current electron beams (HCEB) with different surfaces is now attracting a great deal of attention because of the possibility of employing the effects of the reflection of a beam with compensated charge from a conducting surface for reflecting HCEB at definite angles and also for forming high-current ring-shaped electron beams [1]. In view of the solution of these problems it is of interest to employ the interaction of a beam with a plasma layer. Such systems have the advantage over metallic surfaces that it is possible to compensate comparatively rapidly the space charge of the electron beam either by injecting it into the region of the diffuse boundary of the plasma layer or by means of flow of ions into the region of the beam in the space-charge field of the charge-uncompensated head part of the beam in a sufficiently high vacuum ($1.3\cdot10^{-2}$—$1.3\cdot10^{-3}$ Pa) in the main volume of the drift space.

In this paper we present the results of an experimental and theoretical investigation of the reflection of a high-current electron beam from a plasma layer in order to find the optimal conditions of reflection.

1. The experiments were performed on an accelerator with an electron beam with the following parameters [2]: the energy E_b = 450 keV (γ = 1.9), the current I_b = 10 kA, the radius r_b = 1cm, and the pulse duration t_p = 25 nsec. Two types of plasma layers were used: a) a layer formed with a sliding discharge along the surface of a dielectric (glass 6 mm thick) and b) a layer formed with a discharge between flat parallel electrodes. To reduce the ohmic resistance, copper electrodes were employed in the discharge circuit.

The layout of the experiment is shown in Fig. 1, where 1 and 5 are the receiving and transmitting antennas of the microwave diagnostics, respectively; 2 is a photodiode; 3 is a telescope; 4 is a sectioned Faraday cylinder (SFC); 6 is an electrode; 7 is a dielectric; and, e is the direction of motion of the beam. The discharge was ignited between electrodes whose length was varied in the range 50-250 mm, while the distance between them was constant (60 mm), in the case b the dielectric substrate was removed. The discharge was ignited with the help of a high-voltage pulse with an amplitude of up to 25 kV and a 120 nsec first half-period, generated by a generator based on a TGI-1000/25 thyratron. In order to set the required distance between the beam and the plane of the electrodes the entire system can be moved along the vertical x axis.

The use of a low-inductance pulse generator (without parasitic inductances) and low gas pressures ($p \leq 133.3$ Pa) for igniting the discharge, for which the formation of the channel is delayed owing to the reduction in the collision frequency, was facilitated by the formation of a discharge that was uniform along the electrodes and prevented the discharge from being transferred into the completion stage with the formation of a leader channel. The presence of the dielectric substrate changes the character of the discharge from a corona type to a sliding type, and a more uniform discharge is obtained owing to the distributed surface capacitance of the discharge gap [3].

The space-time characteristics of the plasma layers were measured by three methods: 1) microwave sounding at wavelengths of 3 cm and 4 mm based on suppression of the signal in the waveguide segment filled with the plasma under study; 2) recording the change in the emission of the plasma as a function of time with the help of a telescope and photodiode, which gave a

Tomsk. Translated from Zhurnal Prikladnoi Mekhaniki i Tekhnicheskoi Fiziki, No. 3, pp. 6-12, May-June, 1989. Original article submitted June 9, 1986; revision submitted January 11, 1988.

0021-8944/89/3003-0341$12.50

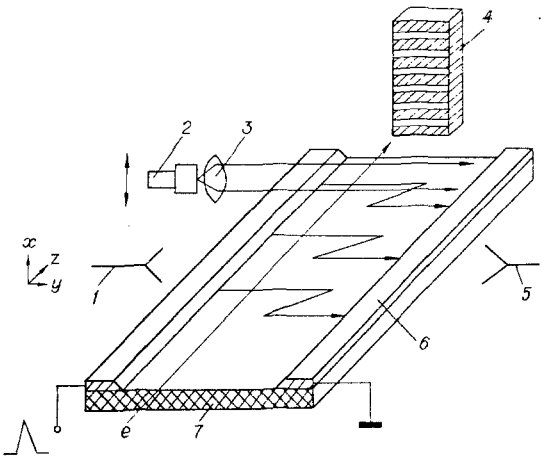

Fig. 1

spatial resolution of 2 mm; and, 3) Langmuir probes were used at the last stages of the decay of the plasma for densities in the range 10^8-10^{12} cm^{-3}. In order to increase the resolution of the microwave sounding of a plasma with a density gradient and to reduce the effect of refraction of radiation on passage of the signal, when the plasma partially fills the transmitting channel, the measurements were performed using two-conductor Lecher wires.

The procedure of obtaining the space–time characteristics consists of the following. For a given distance x the curves of the plasma density as a function of time were constructured from the results of microwave measurements and Langmuir probing, as well as from the curve $I_{em}^{1/2}$. Here I_{em} is the intensity of the plasma emission, which for the parameters studied is determined after termination of the discharge current ($\tau > \tau_d \sim 30$ nsec) is determined by the recombination rate of the ions: $I_{em} \sim \alpha n_e^2$ (α is the recombination coefficient). This procedure was repeated in the entire range of variation of x. After this the curves showing the dependence of the plasma density on x were constructed for different times. The use of these methods simultaneously made it possible to follow the characteristics of the plasma for densities in the range $n_e \sim 10^8$—10^{14} cm^{-3} with a spatial resolution of ~5 mm.

Figure 2 shows the results of measurements of the plasma density distribution along the normal to the plane of the discharge for interelectrode (a) and sliding (b) discharges. The curves 1-4 correspond to the times after the pulse generator is triggered t_0 = 0.2, 1, 3, and 10 μsec. The air pressure in the chamber p = 13.3 Pa. The accuracy with which the plasma density n_e is determined is a function of n_e. The standard deviations for five measurements are presented on the graphs for one curve. The scheme employed to create the plasma layer gives densities of $n_{e\,max} = 10^{14}$ cm^{-3} and an exponential decay length of $\Delta x \sim 0.2$—0.5 cm, over which the density drops by a factor of 2.7. Deformation of the distribution $n_e(t)$, owing to the decay of the plasma, causes n_e to decay and Δx to increase . It follows from Fig. 2b that Δx_{max} is greater for a sliding dischage, since the presence of the dielectric leads to more efficient recombination of the plasma.

The parameters of the beam were monitored with a Faraday cylinder, a Rogowski loop placed at the outlet of the beam from the accelerator, and a small magnetic spectrometer. The coordinates of the center of gravity of the beam after passage through the interaction zone were determined with the SFC or a sectioned scintillation detector with POPOP luminophore, installed instead of the SFC. The electric signals from the sensors were recorded on two 6LOR-04 oscilloscopes, triggered synchronously. The experiments on studying the interaction of the HCEB with the plasma layer were performed in a cylindrical chamber 40 cm in diameter and 15 cm high, into which the beam was injected radially.

Figure 2 also shows the measurements of the transverse force F/F_{max} as a function of the impact parameter $X = x/r_b$ for the interelectrode (c) and sliding (d) discharges with p = 13.3 Pa. The curves were constructed based on measurements of the relative displacement of the center of gravity of the beam $\delta x/\delta z$, where δx is the magnitude of the displacement of the beam along the coordinate x and δz is the extent of the plasma layer corresponding to this displacement. The largest spread in the measurements occurred for $X < 1$ and $X > 3$. For this reason and also taking into account the poor repeatability of the beam parameters each value represented on the graphs is the result of the statistical analysis of the values obtained with five shots of the accelerator.

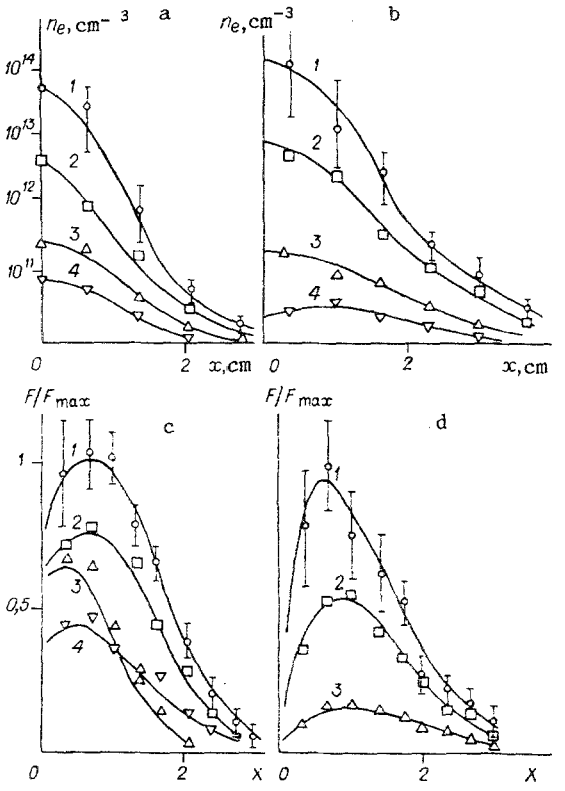

Fig. 2

Figure 2c shows the reflection force as a function of X and the parameters of the plasma layer for an interelectrode discharge with the space-time characteristic n_e (x, r) presented in Fig. 2a. Analysis of the curves shows that in the entire region of the parameters of the experiment the reflection force depends on X in a characteristic fashion: there exists an impact parameter for which the force of reflection is maximum, and as X increases it drops off nearly as X^{-1} and $F \to 0$ as $X \to 0$. The largest effective reflection of the beam occurs at the moment $\tau = 0.2$ μsec corresponding to an end of the discharge pulse, when the plasma density and the gradient of the density at the boundary of the layer are highest. At this time plasma production continues and the recombination process can be neglected.

At $\tau = 1$ μsec the beam is injected into a layer with the more diffuse boundary (Fig. 2a) and the force of reflection becomes substantially weaker; this is especially noticeable at the maximum, when the density gradient affects most strongly the spatial separation of the beam current and the plasma current. For the moment of beam injection $\tau = 3$ μsec because of the strong smearing of the boundary of the plasma layer with the general low level of reflection the force of reflection has a weak maximum and is virtually independent of X. When the injection is further delayed ($\tau = 10$ μsec) no perturbation of the beam trajectory is observed within the experimental error. The curve in Fig. 2a gives in this case $n_{emax} = 7.10^{10}$ cm^{-3}, $\Delta x = 0.4$ cm.

The general characteristics of the dependence of the force of reflection on the plasma density and its gradient at the boundary of the layer are the same for a sliding discharge (Fig. 2d). However the presence of a dielectric substrate, which is an additional source of plasma with injection of a high-current beam [1, 4] in this scheme can change the structure of the plasma layer and the efficiency of beam reflection. This effect affects beam reflection most strongly with low densities of the synthesized plasma; this explains the presence in this scheme of a comparatively high maximum in the force of reflection at $\tau = 3$ and 10 μsec, when, as follows from the corresponding curves in Figs. 2a-c, the decaying synthesized plasma layer cannot give efficient reflection of the beam as well as displacement of the maximum of the force of reflection to the surface of the dielectric. As the density of the synthesized plasma increases the effect of the surface of the dielectric becomes increasingly weaker; for $\tau = 1$ μsec the presence of the dielectric still leads to an appreciable increase in the force of reflection at the maximum (by a factor of ~1.4) and a more rapid dropoff of F (X) than for the interelectrode discharge scheme, whereas for $\tau = 0.2$ μsec (it corresponds in the experiment to more efficient reflection) the dielectric has virtually no effect.

2. Analytical study of the reflection of a charge-compensated high-current electron beam from a plasma layer with a sharp boundary shows that at distances $z_l^2 \ll |z'|^2 \ll z_d^2$ from the beam head in the plasma layer a comparatively high plasma current is induced at the boundary of the layer; the density of this current is given by [5]

$$j_{pz} = 4en_b\gamma_f v_f \frac{r_b^2(f-\tilde{\gamma}^{-2})}{(x_0^2-y^2)^2}\left[(1-\ln 2)(x_0^2-y^2)+\right.$$

$$\left.+2x_0x\left(\ln 2-\frac{1}{2}\right)\frac{x_0^2-3y^2}{x_0^2+y^2}-\frac{\nu_e|z'|\lambda_p^2}{v_f}\frac{x_0^4-6x_0^2y^2+y^4}{(x_0^2+y^2)^2}\right],$$

where $z_\ell = 4(v_0/\nu_e)\,[1-(\lambda_p/r_b)]$ – is the decay length of the surface waves excited in the plasma layer at the front of the beam (usually $z_\ell \lesssim r_b$); $z_d = v_0 r^2{}_b/\nu_e\lambda_p{}^2$ – is the diffusion length of the magnetic field; c is the velocity of light; m_0 is the electron rest mass; e is the elementary charge; $\lambda_p = c/w_p$; $w_p = (4\pi e^2 n_e/m_0)^{1/2}$ is the plasma frequency of the plasma electrons; ν_e is the effective frequency of collisions between plasma electrons and ions and neutrals; n_b and v_0 are the density and average velocity of the beam; $v_f = \beta_f c$ is the velocity of the beam front; $f = n_i/n_b$ is the charge neutralization factor; x_0 is the distance from the beam axis to the boundary of the plasma; $\tilde{\gamma} = (1-\beta_0\beta_f)^{-1/2}$; $\gamma = (1-\beta_0^2)^{-1/2}$; $\gamma_f = (1-\beta_f^2)^{-1/2}$; $\beta_0 = v_0/c$; $z' = z - v_0 t$. At these distances primarily the interaction between the beam current and the induced plasma is manifested, since the induced charge density in the plasma layer is a second-order infinitesimal in the parameter $\nu_e\lambda_p/v_0 \ll 1$ relative to j_{pz}.

The transverse force acting on the average particles of the beam, which lie on the points $x = x_0$ and $y = 0$ along the z axis, arising to the interactions indicated above, has the form in the region $z_\ell^2 << |z'|^2 << z^2{}_d$

$$F(x_0,0,z') = 8\pi e^2 n_b r_b^2 (f-\tilde{\gamma}^{-2})\frac{\beta_0\beta_f\gamma_f}{x_0}\left(0.17-0.2\frac{\nu_e|z'|\lambda_p^2}{4v_f r_0^2}\right), \qquad (2.1)$$

whence it follows that the beam is reflected from the plasma surface more efficiently as n_e increases and the collision frequency decreases. This is attributable to the growth in both the magnitude of the plasma current and its decay length. It also follows from the expression (2.1) that the force of reflection decreases as the impact parameter increases. This dependence on the impact parameter describes well the experimental curves (Fig. 2c) only if the distance between the beam and the plasma layer is significant, when the diffuseness of the boundary of the layer can be neglected.

To study the effect on the efficiency of beam reflection from a plasma layer with a diffuse boundary the passage of a HCEB near a plasma layer with a diffuse boundary was studied using the method of numerical modeling. To describe the physical mechanism the following equations were employed in the numerical model:

$$\frac{4\pi}{c}\sigma(x)\frac{\partial A_z}{\partial t}-\frac{1}{\nu_e}\frac{\partial^3 A_z}{\partial t\,\partial x^2}-\frac{\partial^2 A_z}{\partial x^2}=\frac{4\pi}{c}\left(j_b+\frac{1}{\nu_e}\frac{\partial j_b}{\partial t}\right),$$

$$\frac{1}{\nu_e}\frac{\partial j_{pz}}{\partial t}+j_{pz}=-\frac{\sigma(x)}{c}\frac{\partial A_z}{\partial t},$$

$$F(x=x_0)=e\frac{v_{bz}}{c}B_y(x=x_0),\quad f=1,$$

where A_z is the axial component of the vector potential, satisfying zero boundary conditions and initial conditions; j_b is the current density of the injected beam; $\sigma(x)$ is the conductivity of the plasma; v_{bz} is the average velocity of the beam of electrons taking into account the retardation of the electrons in teh induced field E_z at the front of the beam, calculated from the average losses over the interaction length $\Delta E_b = |eE_z L_z|$. For relativistic particles with $\beta_0 \sim 1$ and actually existing currents $v_{bz} \sim v_0$ At the moment of injection $t = 0$ ($\tau = t + t_0$).

The pulse of current in the beam as a function of time $I_b(t)$ was chosen to be a trapezoid with the corner points approximated by third-order curves and the plasma density was taken in the form $n_e(x) = 2n_{0e}\left[1+\exp\left(\frac{x-x_1}{\Delta x}\right)\right]^{-1}$, which corresponded to the experimental measurements (Fig. 2a).

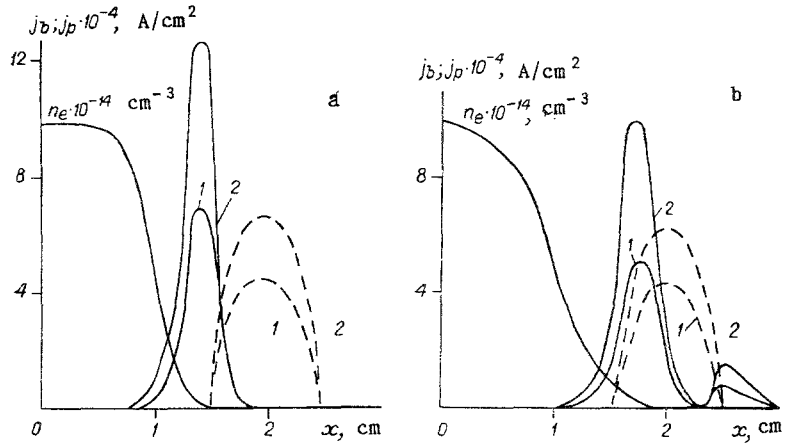

Fig. 3

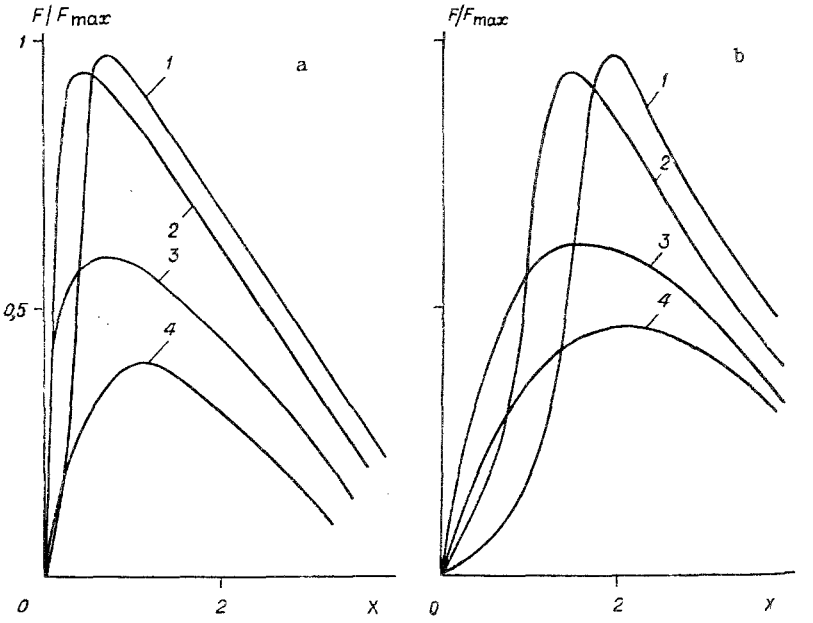

Fig. 4

The results of the numerical calculations are presented in Figs. 3 and 4. Figures 3a and b (Δx = 0.1 and 0.2 cm, respectively) show the dependence of the current distribution in the beam $j_b(z)$ (broken lines) and the plasma current $j_p(z)$ (solid lines) on the depth of the plasma layer with I_b = 30 kA and $n_{0e} = 10^{15}$ cm^{-3} (the lines 1 and 2 for t = 8 and 15 nsec). The curves show that when the density gradient (a) is large practically all of the plasma current flows outside the beam and the transverse force acting on the beam is sufficient to change the trajectory of the beam; as the gradient of $n_e(x)$ decreases (the smearing increases) part of the plasma current flows in the region of the beam (b) and the force of reflection becomes weaker.

Figure 4 shows the force of reflection F/F_{max} as a function of the impact parameter for p = 13.3 (a) and 66.5 Pa (b); the curves 1-4 correspond to $n_{0e} = 5.2 \cdot 10^{13}$; $6.3 \cdot 10^{12}$; $5.1 \cdot 10^{11}$; $1.9 \cdot 10^{11}$ cm^{-3} with I_b = 10 kA. The behavior of the curves and analysis of the calculations show that for each plasma density there exists an impact parameter X_{max} for which the plasma current leaves the region of the beam and the force of reflection is maximum. This effect – a consequence of the diffuseness of the boundary – is explained by the fact that as the impact parameter decreases part of the plasma current flows in the region of the beam, which sharply weakens the force of interaction of the currents, and as the impact parameter increases the force of reflection decreases owing to the increase in the distance between the interacting currents. In the process the rate of decrease of the force reflection as the impact parameter increases depends on the degree of diffuseness of the boundary and for a sufficiently sharp boundary (curve 1) the dependence

$F(X)$ for $X > X_{max}$ is close to the analytical dependence (2.1). The presence and position of a maximum in the theoretical dependence of the force of reflection on X agree with the behavior of the experimental curves in Fig. 2c.

Changing the pressure of the residual gas in the chamber with high plasma density has virtually no effect on the profile of the reflection forces as long as the conductivity of the plasma in the region of injection is determined primarily by the electronic collisions and the ionization of the gas by the beam is still insignificant.

In this case the maximum of reflection shifts, owing to avalanche ionization at the front of the beam, toward increasing impact parameter (Fig. 4b). For a low plasma density, when collisions with neutrals play an appreciable role, the efficiency of reflection changes strongly with the gas pressure and drops rapidly as the gas pressure is increased. The analytical and computed dependence obtained for the force of reflection supplement one another and agree well with the experimental measurements over a wide range of impact parameters $X > 0.4$, encompassing the range of most efficient reflection.

The theoretical and experimental results presented show that reflection of the beam from the types of plasma layers studied occurs in virtually the same manner when the density of the synthesized plasma is sufficiently high. When the plasma density decreases, a difference is observed in the systems. In this case, for small impact parameters, reflection is more efficient in the presence of a dielectric substrate than when there is no dielectric. This is explained by the beam-induced formation of a plasma near the wall at the surface of the dielectric – this increases the gradient of n_e.

Comparing the results obtained with the results on reflection from metallic surfaces [1] leads to the conclusion that in the optimal regime (high plasma density and high gradient $|\partial n_e/\partial x|$) for impact parameters $X \geq X_{max}$ the character of the dependence of the force reflection on X and its magnitude do not differ significantly from the force of reflection in the case of a metallic surface.

Since in the case when a beam is reflected from metallic surfaces it is difficult to meet simultaneously the requirements that the charge of the beam be compensated and that there be no plasma with high conductivity in the region of the beam [6], it is more efficient to use reflection systems based on the plasma layers enabling control of the plasma current.

LITERATURE CITED

1. A. N. Didenko, V. P. Grigor'ev, and Yu. P. Usov, Powerful Electron Beams and Their Applications [in Russian], Atomizdat, Moscow (1977).
2. R. A. Akopov, O. G. Antablyan, and E. K. Khanikyants, "Propagation of high-current electron beams in curved dielectric channels," Izv. Akad. Nauk ArmSSR, Fiz., 18, No. 2 (1983).
3. S. I. Andreev, E. A. Zobov, et al., "Investigation of long sliding spark," Zh. Prikl. Mekh. Fiz., No. 1 (1980).
4. R. A. Akopov, O. G. Antablyan, et al. "Investigation of IREP with a dielectric surface," Zh. Tekh. Fiz., 56, No. 3 (1986).
5. V. P. Grigor'ev, A. N. Didenko, and G. P. Isaev, "Injection of compensated relativistic electron beams near a plasma half-space," Fiz. Plazmy, 9, No. 6 (1983).
6. A. V. Petrov, S. A. Pechenkin, et al., "Investigation of mirror capture of a high-current relativistic electron beam in a closed, " Tr. Nauchno-Issled. Inst. Yad. Fiz., Atomizdat, Moscow (1979), No. 8.